

Renormalization-group approach to the problem of light-beam self-focusing

V. F. Kovalev

Institute for Mathematical Modelling, Russian Academy of Science, Moscow 125047, Russia

V. Yu. Bychenkov

P. N. Lebedev Physics Institute, Russian Academy of Science, Moscow 117924, Russia

V. T. Tikhonchuk*

Department of Physics, University of Alberta, Edmonton, Canada T6G 2J1

(Received 26 May 1999; published 14 February 2000)

A method of renormalization-group symmetries is applied for analytical solution to the nonlinear Schrödinger equation which describes the electromagnetic beam self-focusing in a medium with a cubic nonlinearity. The boundary-value problem for the incident Gaussian light beam has been solved analytically in a cylindrical geometry although the method could be applied to other boundary conditions too. The solution describes a detailed structure of wave self-focusing and its global characteristics such as the light power trapped in the singularity, laser beam radius, and self-focusing length. A comparison with the results of previous studies demonstrates advantages of the renormalization-group symmetry method as a tool for the nonlinear electro-dynamics theory.

PACS number(s): 42.65.Jx, 42.65.Tg, 02.20.-a, 52.35.Mw

I. INTRODUCTION

The problem of self-focusing of a high-power light beam [1–5] plays an important role in nonlinear electrodynamics since the early 1960s. As a detailed quantitative understanding of self-focusing is still far away, a search for effective ways of its analytic description is an ongoing concern. For example, self-guiding of an intense laser pulse in an underdense plasma for many Rayleigh lengths without significant losses has been demonstrated many times both experimentally and in numerical simulations [6–8]. However, there is no parametric scaling for the laser beam power trapped in a self-focused channel. A mathematical model of wave self-focusing is based on the nonlinear Schrödinger (NLS) equation for the complex amplitude of the electric field E of electromagnetic beam:

$$2ik_0\partial_z E + \Delta_{\perp} E + k_0^2(\epsilon_2/\epsilon_0)E = 0, \quad E(0, \mathbf{r}) = E_0(\mathbf{r}). \quad (1)$$

It describes a stationary beam propagation in the direction z with an assumption that the wave-amplitude scale length along the z axis is much larger as compared to the characteristic scale in the transversal direction. Here, $k_0 = (\omega/c)\sqrt{\epsilon_0}$ is the wave number, Δ_{\perp} is the Laplace operator in the perpendicular plane \mathbf{r} , and ϵ_0 and ϵ_2 are the real parts of linear and nonlinear dielectric permittivities, respectively. Regular and explosivelike singular solutions to Eq. (1) have been investigated by using various analytical and numerical methods. However, none of the analytical methods is able to provide an exact solution to the NLS equation for arbitrary boundary conditions. Only some specific boundary value problems (BVPs) that are far away from practical requirements have been solved analytically so far.

The studies of stationary light-beam self-focusing may be attributed to the following three categories. The first category includes rigorous analytical theories such as the inverse-scattering method [9] and the classical group analysis [10,11]. Approximate analytical methods, such as the paraxial ray (nonaberrational) approach [3,4,12], the method of moments [13], the variational theory [14], and modifications of the inverse-scattering method which employ asymptotic [15] or perturbation [16] expansions, constitute the second category. The third group enrolls various numerical methods reviewed in Ref. [17]. The present paper falls into the first and partly, the second category. It deals with an application of a method [18] of renormalization-group symmetries (RGS) for the solution of a NLS equation.

A common disadvantage of rigorous mathematical methods is that they consider some special solution for a specific BVP. The inverse-scattering method has been developed for a planar geometry and for a cubic nonlinear medium. It is designed for the derivation of single- and multiple-soliton NLS solutions [9,19]. Two ameliorations to the inverse-scattering method have been proposed for the description of the radiation fields that may accompany the formation of a self-guided channel. One of them is based on a perturbative approach [16,20] and another on an asymptotic expansion [15]. However, both methods inherited the same restrictions to the BVP solution as the basic inverse-scattering method. A large variety of exact solutions to the NLS equation in one-dimensional (1D), two-dimensional (2D), and three-dimensional (3D) geometry for cubic and quintic nonlinearity and with additional linear inhomogeneous terms have been obtained in Refs. [10,11,21] by using the symmetry groups. However, boundary conditions for these solutions do not correspond to a localized electromagnetic beam at the entry plane.

Approximate methods are relatively simple and flexible. They have been applied to a qualitative description of light-beam self-focusing for a cubic and saturating nonlinearity

*On leave from P. N. Lebedev Physics Institute, Russian Academy of Science, Moscow 117924, Russia.

[22–24]. A weak point of approximate methods is in *a priori* assumption about the light beam radial structure. The paraxial ray approximation [3,4,25,26] is restricted to a small vicinity near the beam axis. The variational method [14,27] involves a set of self-similar trial functions that describe light-beam radial distribution with a few z -dependent parameters (wave amplitude, beam width, and phase front curvature). They satisfy the equations that follow from minimization of the basic functional. For the NLS equation with a cubic nonlinearity both paraxial ray and variational methods describe the beam behavior from the entrance boundary up to a singularity point where the beam intensity tends to infinity and the beam width turns to zero. However, numerical simulations for the Gaussian incident beam demonstrate a significant modification of the radial beam profile near the singularity point: a narrow spike with a very large intensity on the beam axis was found in Ref. [28]. This is in striking contrast to the self-similar beam structure prescribed by the approximate methods. A modification of the method of moments that has been proposed in Ref. [13] does not imply *a priori* assumption on the light-beam structure. It could provide better description of the beam behavior near the singularity, but no analytical results have been obtained so far. There is also an unexplained four times difference in the value of the critical power predicted by the paraxial ray theory [29] and the method of moments [13].

The numerical simulations of the light-beam self-focusing [2,17,30–35] bear two main difficulties. First, they do not define parametric scaling for a number of the input beam characteristics as the radial shape, power, and phase front curvature. Second, they cannot describe the beam behavior in the vicinity of singularity with sufficient accuracy [33,36]. Singular solutions for various space dimensions and different types of nonlinearity have been derived in Refs. [36–39]. For a medium with the cubic nonlinearity a class of quasi-self-similar solutions has been found where z -coordinate dependence of the electric-field intensity near the singularity point z_s exhibits the dependence $L(z)/(z-z_s)$ [36,39] with a slowly varying double logarithmic function $L(z) \sim |\log \log(z-z_s)|$ [39–42]. However, another exact collapsing solution to the NLS equation has been constructed in [43] where the intensity enlarges to $1/(z-z_s)^2$.

Thus, more than 30 years of studying self-focusing has not been crowned with success in constructing a method that allows us to find an analytical solution to the NLS equation with arbitrary boundary conditions. There are also a number of contradictions between different theories which have not been resolved yet. A parametric analysis of global self-focusing characteristics versus boundary conditions is still far away from its applications. In this paper we present a rather general method for finding analytical solutions to the NLS equation by using the RGS approach. The paper is organized as follows: In Sec. II the RGS method is formulated for a cylindrical light beam. This method is applied to a BVP problem with a Gaussian beam profile at the entrance boundary in Sec. III. Global characteristics of self-focusing are considered in Sec. IV and compared with results of previous publications. Our results are summarized in Sec. V.

II. APPLICATION OF THE RGS METHOD FOR A NLS EQUATION FOR THE AXIALLY SYMMETRIC CASE

The key idea of our approach to the solution of a NLS equation consists of finding a special class of symmetries for the chosen BVP [18]. These symmetries involve a group of invariant transformations of dependent and independent variables and parameters defining the solution. For a given RGS, the required BVP solution can be obtained by using a finite group transformation which associates a complex field amplitude inside a nonlinear medium with its boundary value.

Long before the idea of applying RGS as a practical tool for the solution of BVP in mathematical physics had been formulated, the renormalization-group transformations had been used in the quantum field theory [44] to improve approximate solutions. The concept of renormalization-group transformations had also been applied to some areas of microscopic physics for description of phase transitions in large statistical systems like spin lattices and polymers [45], and to some problems of macroscopic physics like transport theory, hydrodynamics, and turbulence [46]. Having the same goal to improve the perturbation theory and to simplify the analysis of a singular behavior of a solution, the ideas of the renormalization-group method have been introduced in mathematical physics. An exact group of point transformations has been used in a plasma theory [47] to find a strongly nonlinear BVP solution to the system of equations that describe wave harmonics generation starting from a perturbative solution. Methods of quantum field theory and the Wilson's renormalization-group have also been applied for the asymptotic analysis of nonlinear parabolic equations, which describe surface gravitational waves in liquids, shock waves dynamics, and radiative heat transport [48,49]. Recently the perturbative renormalization-group theory [50] has been developed for a global asymptotic analysis.

The regular RGS method [51,52] involves a functional self-similarity and algorithms of modern group analysis. It does not imply any *a priori* assumptions and provides an approximate analytical solution to a specific BVP. The RGS method has been applied for the analysis of a number of particular solutions of BVP in nonlinear optics [53–57]. However, there was no universal algorithm of finding renormalization-group transformations until recently when a general RGS approach had been derived in Ref. [18] for systems of differential equations. Depending on a mathematical model and boundary conditions, the procedure of finding RGS can be accomplished in different ways. For finding a solution to the NLS equation we employ the algorithm of approximate symmetries [58] for systems of differential equations with small parameters. For Eq. (1) these small parameters are the nonlinearity, $\alpha = \epsilon_2(I_0)/2\epsilon_0$, and the diffraction, $\beta = 1/2k_0^2 r_0^2$, where I_0 is the characteristic intensity of the laser beam at the boundary and r_0 is the initial beam radius. Both parameters can be made arbitrarily small if one considers a converging beam and the entrance plane far away from the focal position.

We consider a cylindrically symmetric electromagnetic beam incident at $z=0$ on a homogeneous medium with a cubic nonlinearity, $\epsilon_2(I) = \gamma I$. The electric field, $E = \sqrt{I} \exp(ik\Psi)$, is represented in terms of two real functions:

the intensity I and the phase Ψ , which satisfy the system of two equations:

$$\partial_z k + k \partial_r k - \alpha \partial_r I - \beta \partial_r \left[\frac{1}{r\sqrt{I}} \partial_r (r \partial_r \sqrt{I}) \right] = 0, \quad (2)$$

$$\partial_z I + I \partial_r k + k \partial_r I + kI/r = 0.$$

Here, $k = \partial_r \Psi$ is the radial phase derivative, both coordinates r and z are normalized by the initial beam radius r_0 , and the intensity is normalized by the on-axis intensity I_0 at the entrance plane. The boundary conditions,

$$I(0,r) = I_0 N(r), \quad k(0,r) = -r/R, \quad (3)$$

assume that the incident beam intensity is an arbitrary function of the radius, $N(0) = 1$, and that the incident beam has a spherical front, $\Psi(0,r) = -r^2/2R$, where R is the radius of the wavefront curvature ($R > 0$ for a converging beam and $R \rightarrow \infty$ corresponds to a collimated beam).

The key point in finding the BVP solution is to construct the RGS. For that purpose, following the general RGS theory [56,59], we use the Lie-Bäcklund symmetries admitted by original differential equations (2) and determined by the canonical group operator $\hat{X} = f \partial_k + g \partial_I$. The coordinates f and g of this operator are found by solving the corresponding determining equations expressing the invariance conditions for system (2) with respect to the group with the operator \hat{X} . We expand f and g in power series over the nonlinearity and diffraction parameters

$$f = \sum_{i,j=0} \alpha^i \beta^j f_{ij}, \quad g = \sum_{i,j=0} \alpha^i \beta^j g_{ij}, \quad (4)$$

where the coefficients f_{ij} and g_{ij} are functions of z , r , k , and I and of arbitrary-order derivatives of k and I with respect to r . Substituting Eq. (4) into the determining equations and comparing the coefficients in powers of α and β one can find a system of equations for coefficients. We consider here only low order equations, which are independent on α and β and which are linear over α or β . This is justified if the coordinates f and g contain only linear contributions with respect to the parameters α and β or the values of these parameters are small. In the latter case, the neglect of higher-order terms means that we are finding an approximate symmetry.

The coordinates f and g depend on a set of arbitrary functions that can be defined by the group restrictions. By using the invariance condition, $f = 0$, $g = 0$, for the particular BVP solution and requesting the compatibility between this condition and the prescribed boundary data (3), we obtain the following RGS operator:

$$\left\{ f = D_r \frac{1}{2R^2} \left[r + kR \left(1 - \frac{z}{R} \right) \right]^2 - \left(1 - \frac{z}{R} \right)^2 \left[\alpha I + \frac{\beta}{r\sqrt{I}} D_r (r D_r \sqrt{I}) \right] + S \right\}, \quad (5)$$

$$g = \frac{1}{r} D_r \left\{ r I \left[\frac{1}{R} \left(1 - \frac{z}{R} \right) (r + kR - kz) - z \partial_\chi S \right] \right\}.$$

Here, D_r is the operator of total differentiation with respect to r ,

$$D_r \equiv \partial_r + \sum_{s=0}^{\infty} (k_{s+1} \partial_{k_s} + I_{s+1} \partial_{I_s}) \quad (6)$$

where $k_s = \partial_r^s k$ and $I_s = \partial_r^s I$ are the corresponding partial derivatives and the function S depends on $\chi = r - kz$ and two expansion parameters,

$$S(\chi) = \alpha N(\chi) + \frac{\beta}{\chi \sqrt{N(\chi)}} \partial_\chi [\chi \partial_\chi \sqrt{N(\chi)}]. \quad (7)$$

The following point renormalization-group operator is equivalent to the canonical renormalization-group operator with coordinates (5):

$$\begin{aligned} \hat{X} = & \left[\left(1 - \frac{z}{R} \right)^2 + z^2 S_{\chi\chi} \right] \partial_z + \left[\frac{r}{R^2} + \frac{k}{R} \left(1 - \frac{z}{R} \right) + S_\chi \right] \partial_k \\ & + \left[-\frac{r}{R} \left(1 - \frac{z}{R} \right) + z S_\chi + kz^2 S_{\chi\chi} \right] \partial_r + \left[\frac{2I}{R} \left(1 - \frac{z}{R} \right) - Iz \left(1 + \frac{kz}{r} \right) S_{\chi\chi} - \frac{Iz}{r} S_\chi \right] \partial_I. \end{aligned} \quad (8)$$

Operator (8) serves as a tool for finding solutions of the desired boundary value problem. It describes the finite-group transformation that relates the values of the beam intensity and phase for any $z > 0$ to the prescribed data at the boundary:

$$k(z,r) = \frac{r - \chi}{z}, \quad I(z,r) = N(\mu) \left(1 - \frac{z}{R} \right)^{-1} \frac{\chi}{r} \frac{\partial_\chi^2 S}{\partial_\mu^2 S}. \quad (9)$$

The dependence of two additional functions, χ and μ , on z and r is defined by the following relations:

$$\begin{aligned} r = & \chi \left(1 - \frac{z}{R} \right) \left[1 + \frac{2z^2 \partial_\chi^2 S}{(1 - z/R)^2} \right], \\ S(\mu) - S(\chi) = & \frac{z^2 (\partial_\chi S)^2}{2(1 - z/R)^2}. \end{aligned} \quad (10)$$

It is important to note that the solution (9) has been derived with no *a priori* assumptions concerning the spatial structure of beam inside the medium $N(r)$. The perturbative approach used to find RGS does not impose significant restrictions on Eq. (9) because physically the focal point, $z \approx R$, can be placed far away from the input boundary. A good accuracy of solutions given by the RGS method has already been demonstrated for the nonlinear geometrical optics equations ($\beta = 0$) in Ref. [56].

III. BOUNDARY VALUE PROBLEM SOLUTION FOR A GAUSSIAN BEAM

We analyze the general features of Eqs. (9) and (10) for a Gaussian intensity profile, $N(r) = \exp(-r^2)$. According to Eq. (7), $S(\chi) = \alpha \exp(-\chi^2) + \beta(\chi^2 - 2)$, and the beam structure can be written from Eqs. (9) as follows:

$$k(z, r) = \frac{r - \chi}{z}, \quad I(z, r) = e^{-\mu^2} \left(1 - \frac{z}{R}\right)^{-1} \frac{\chi}{r} \frac{\beta - \alpha e^{-\chi^2}}{\beta - \alpha e^{-\mu^2}}, \quad (11)$$

where the parameters χ and μ are defined by the relations

$$\beta(\mu^2 - \chi^2) + \alpha(e^{-\mu^2} - e^{-\chi^2}) = 2z^2 \chi^2 \frac{(\beta - \alpha e^{-\chi^2})^2}{(1 - z/R)^2}, \quad (12)$$

$$r = \rho(z, \chi) \equiv \chi \left(1 - \frac{z}{R}\right) \left[1 + 2z^2 \frac{\beta - \alpha e^{-\chi^2}}{(1 - z/R)^2}\right].$$

In the linear limit, $\alpha = 0$, Eqs. (11) and (12) describe exactly the well-known solution for a Gaussian beam in a linear medium (cf. Ref. [29] [Sec. 22]):

$$I(z, r) = \frac{1}{w^2} \exp\left(-\frac{r^2}{w^2}\right), \quad k(z, r) = -\frac{r}{R} \frac{1 - (z/R)(1 + 2\beta R^2)}{w^2}, \quad (13)$$

where $w(z) = \sqrt{(1 - z/R)^2 + 2\beta z^2}$ is the effective beam radius. The beam with $R > 0$ converges up to the focal plane at $z = z_f = R/(1 + 2\beta R^2)$, where the rays¹ become parallel to the beam axis. The focal plane is also a plane of turning points, i.e., the place where $k = 0$. Therefore, all rays turn away from the z axis in the same plane. In the focal plane the beam radius achieves its minimum, $w_{min} = 1/\sqrt{1 + 1/2\beta R^2}$. Another important parameter of the linear theory is the Rayleigh length, $L_R = w_{min}^2/\sqrt{2\beta}$, which is a distance from the focal plane to the plane where the beam intensity decreases two times.

In the nonlinear case turning points do not belong to the focal plane any more. Different rays turn away from the axis at different positions and the curve of turning points, $r_t(z)$, is defined by the following equation (assuming $\alpha < \beta$):

$$r_t^2 = \ln \frac{2\alpha z R^2}{z(1 + 2\beta R^2) - R}. \quad (14)$$

It follows from the condition $r_t > 0$ that this curve is defined only for the interval $z_l < z < z_{nl}$, between the linear and nonlinear focal planes. According to Eq. (14), all turning points

¹The ray direction at a given point is defined by the normal to the phase front surface.

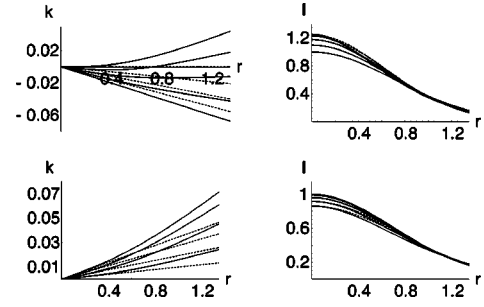


FIG. 1. Radial profiles of the light beam phase gradient and intensity at axial positions $z=0, 1, 2, 3, 4$ in a nonlinear medium with $\alpha=0.005$ and $\beta=0.01$. Dashed lines demonstrate results of the paraxial ray theory. The upper row corresponds to a converging beam, $R=20$, and the bottom panels correspond to a collimated beam, $R \rightarrow \infty$. The distance increases for curves from bottom to top on both panels for k and on the upper panel for I . The distance increases from top to bottom on the bottom panel for I .

lay behind the linear focal plane. The rays that originate at larger distances from the beam axis turn away closer to the linear focal plane. The nonlinear focal plane, $z_{nl} = R/[1 + 2(\beta - \alpha)R^2]$, is defined as a position of the maximum beam intensity,

$$I_{max} = 1 + \frac{1}{2(\beta - \alpha)R^2}. \quad (15)$$

Such a consideration is valid for a weak nonlinearity, $\alpha < \beta$. In the limit $\alpha \rightarrow \beta$ the beam intensity on the axis turns to infinity at $z = R$. For a collimated beam, $R \rightarrow \infty$, the rays always diverge behind the entrance plane, provided $\alpha < \beta$. The radial dependence of k and I for several cross sections and the contour plots of k and I in the (z, r) plane are shown in Figs. 1 and 2, correspondingly, for a converging and collimated beam for the case $\alpha < \beta$. The Rayleigh length in both examples is approximately 7. The paraxial ray theory is in agreement with the RGS solution near the beam axis, $r \lesssim 0.2$, while at larger distances the wave front is stronger bent. The maximum intensity position in the case of converging beam is moved due to the nonlinearity from $z_f = 2.2$ to $z_{nl} = 4$ where the intensity increased in 1.25 times in accordance with Eq. (15).

The case of a stronger nonlinearity, $\alpha > \beta$, is where the nonlinearity dominates diffraction. It requires more thoughtful analysis. The dependence of r upon χ and, therefore, the dependence of k on r that is given by Eqs. (11) and (12) is not a single-valued function for the entire range of z any more. The ambiguity turns on provided two conditions for the function $\rho(\chi)$ are satisfied,

$$\partial_{\chi} \rho = 0, \quad \partial_{\chi\chi} \rho = 0. \quad (16)$$

These two equations reduce in fact to a quadratic equation for the coordinate z , and the position of ambiguity zone depends on the curvature radius of the incident beam. For a large wave-front radius, $R > R_{min} = 1/\sqrt{2(\alpha - \beta)}$, the ambiguity region starts from $z_{f1} = R/[1 + R\sqrt{2(\alpha - \beta)}]$ and extends to infinity. The beginning of the ambiguity region, z_{f1} , corresponds to the position of beam singularity found in the paraxial ray approximation [29].

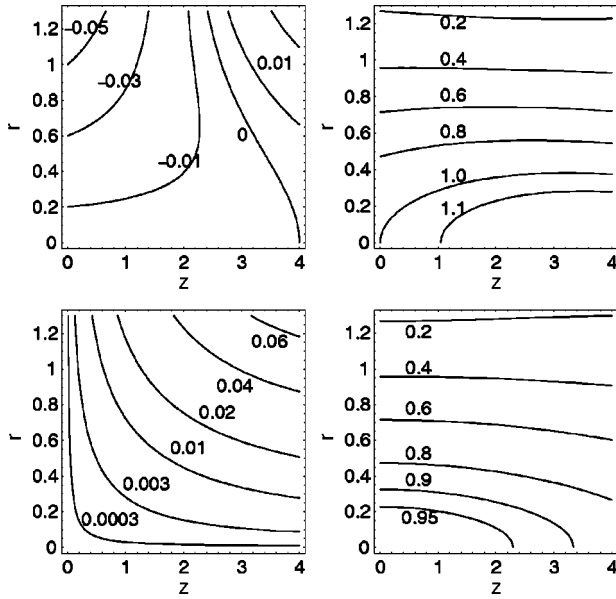


FIG. 2. Contour plots of k and I in the (z, r) plane in a nonlinear medium with $\alpha=0.005$ and $\beta=0.01$ for $R=20$ (upper panels) and $R=\infty$ (bottom panels). The curves are marked by the magnitudes of k and I , correspondingly.

For a tighter focused beam, $R < R_{min}$, the ambiguity region has a finite extent along the propagation axis, $z_{f1} < z < z_{f2}$, where $z_{f2} = R/[1 - R\sqrt{2(\alpha - \beta)}]$ is the second root of Eqs. (16). The length $\Delta z = z_{f2} - z_{f1}$ of the ambiguity region

$$\Delta z = \frac{2R^2\sqrt{2(\alpha - \beta)}}{1 - 2(\alpha - \beta)R^2} \quad (17)$$

increases with the wave-front curvature.

The radius of the ambiguity region Δr depends on the coordinate z ,

$$\Delta r = -\frac{4\alpha z^2}{1 - z/R} \chi_{max}^3 e^{-\chi_{max}^2}, \quad (18)$$

where $\chi_{max}(z)$ corresponds to the local maximum of the function $\rho(z, \chi)$ and follows from the first relation in Eq. (16),

$$\left(1 - \frac{z}{R}\right)^2 + 2z^2[\beta + \alpha(2\chi_{max}^2 - 1)e^{-\chi_{max}^2}] = 0. \quad (19)$$

According to these equations, the radius of the ambiguity region equals zero at the beginning, $z = z_{f1}$, increases with z up to $z = R$, and then decreases to zero at $z = z_{f2}$, provided $R < R_{min}$. The radius Δr goes to infinity for $z \rightarrow R$. That can be seen from Eq. (19) because χ_{max} has a finite value at $z = R$. Although the present solution cannot be extended beyond this point, several conclusions of a physical significance can be drawn for the region $z < R$.

One can find the behavior of a NLS solution in the vicinity of a singularity point z_{f1} . It follows from Eqs. (11) and (12) that the electric-field structure on the axis for $z < z_{f1}$ is defined by the formula

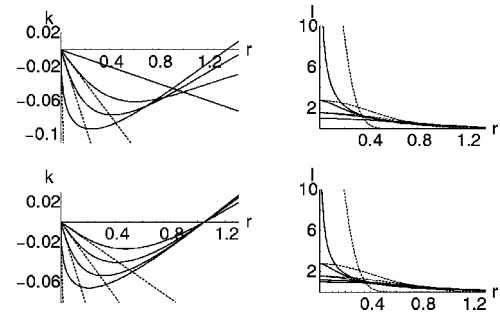


FIG. 3. Radial profiles of k and I for $z=0, 1, 2,$ and 3.9 ($R=20$, upper panels) and $0, 2, 3, 4,$ and 4.9 ($R=\infty$, bottom panels) in a nonlinear medium with $\alpha=0.03$ and $\beta=0.01$. The distance increases for curves from top to bottom on both panels for k and from bottom to top on both panels for I .

$$I(z, 0) = \frac{z_{f1}z_{f2}}{(z_{f1} - z)(z_{f2} - z)}, \quad k(z, 0) = 0, \quad (20)$$

which describes an explosive intensity growth near the singularity point $z = z_{f1}$. At this axial position Eqs. (11) and (12) demonstrate a fractional power radial dependence of I and k near the axis ($r \rightarrow 0$)

$$I(z_{f1}, r) = \frac{(R/r)^{2/3}}{[2\alpha z_{f1}^2(R - z_{f1})^2]^{1/3}},$$

$$k(z_{f1}, r) = \frac{r}{z_{f1}} \left[1 - \left(\frac{1 - z_{f1}/R}{2\alpha r^2 z_{f1}^2} \right)^{1/3} \right].$$

According to these equations, the intensity depends on the radial coordinate as $r^{-2/3}$ and the derivative $\partial_r k$ goes to infinity at the axis. The spatial distributions of k and I for focused and collimated beams for the case $\alpha > \beta$ are shown in Figs. 3 and 4 before the singularity, $z < z_{f1}$. The convergent beam with $R=20$ is expected to have a singularity at $z_{f1}=4$ while $z_{f1}=5$ for the collimated beam. The wave front has a complicated structure: its central part, $r \leq 0.2$, converges in agreement with the paraxial ray theory, while the exterior part of the beam, $r \geq 1$, diverges and does not participate in self-focusing. One can see a significant difference between the exact theory and the paraxial ray theory.

Singularities in the beam intensity and phase derivative indicate the mathematical model based on the NLS equation with a cubic nonlinearity is not complete. There are a number of physical effects which may resolve that singularity. Those are the nonlinearity saturation [60], nonlinear absorption [61], nonlocal nonlinearity [62], etc. The RGS method allows us to solve the BVP problem for NLS equation with an arbitrary nonlinearity and provides an appropriate algorithm to derive such solutions. This could be performed in the future. However, the NLS equation with a cubic nonlinearity has its own merits, and it is of general interest to consider the beam characteristics following from Eqs. (11) and (12) in the ambiguity region by using some plausible physical assumptions.

To resolve the ambiguity we restrict ourselves to consideration of the region $z < R$ and postulate that there are no

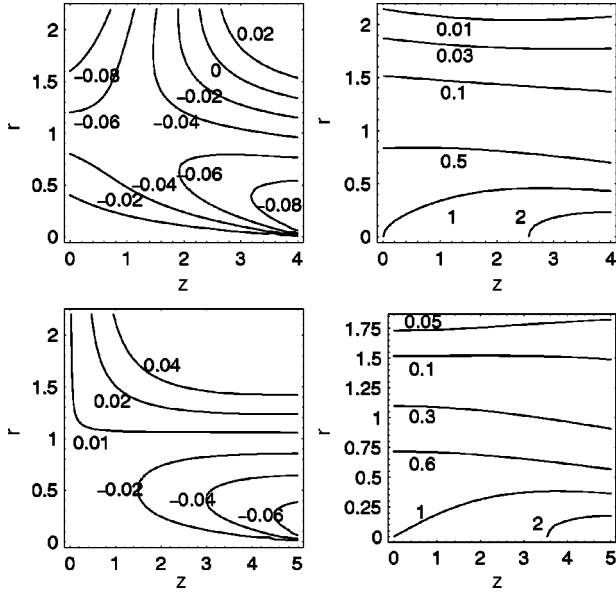


FIG. 4. Contour plots of k and I on the (z, r) plane in a nonlinear medium with $\alpha=0.03$ and $\beta=0.01$ for $R=20$ (upper panel) and $R\rightarrow\infty$ (bottom panel). The curves are marked by the magnitudes of k and I , correspondingly.

rays intersecting the beam axis. This assumption means that all rays approaching the singularity continue their path parallel to the beam axis; in other words, they constitute a channel of a trapped light. Mathematically this assumption corresponds to the condition $\chi > \chi_b$, where $\chi_b = 0$, if $z < z_{f1}$, and

$$\chi_b^2 = \ln \frac{2\alpha z^2}{2\beta z^2 + (1-z/R)^2} \quad \text{if } z_{f1} < z < R. \quad (21)$$

Such a picture of channel formation is similar to the structure described in Ref. [36] where it was called a ‘‘distributed collapse.’’ It also agrees with the results of numerical simulations [28] where the formation of a narrow spike (solution singularity) has been observed on the beam axis.

The radial dependence of intensity near the beam axis, $r \rightarrow 0$ (and, consequently, $\chi \rightarrow \chi_b$), follows from Eqs. (11) and (12) for $z_{f1} < z < R$:

$$I(z, r) = \frac{\chi_b e^{-\mu^2}}{\alpha e^{-\mu^2} - \beta} \frac{R-z}{2Rz^2 r},$$

$$\beta \mu^2 + \alpha e^{-\mu^2} = \left[\beta + \frac{(R-z)^2}{2R^2 z^2} \right] (1 + \chi_b^2). \quad (22)$$

Near the right boundary, $z \rightarrow R$, where $\chi_b^2 \approx \ln(\alpha/\beta)$, the beam intensity can be written explicitly, $I(R, r) = \sqrt{\beta}/2R\alpha r$. It is important to note that such a dependence (22) is valid only in a narrow vicinity of the axis where μ can be considered as a constant. For larger r the beam intensity sharply decreases proportional to $\exp(-\mu^2)$. The function $\mu(z, r)$, according to Eq. (12), becomes large at very small distances from the axis. Hence, the whole beam converges to the axis at $z \rightarrow R$. For a collimated beam, $R \rightarrow \infty$, such a conversion occurs at $z \rightarrow \infty$.

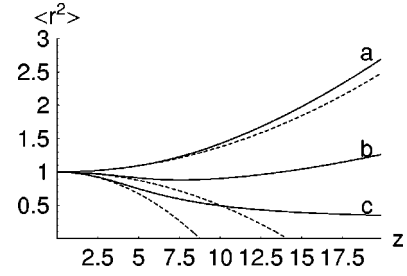


FIG. 5. Axial dependence of the mean square radius $\langle r^2 \rangle$ (solid curve) for a collimated beam ($R \rightarrow \infty$) in a nonlinear medium with $\alpha=0.03$ and $\alpha/\beta=3.2$ (a), 6 (b), and 30 (c). Dashed curves demonstrate the same dependence that follows from the method of moments.

IV. GLOBAL SELF-FOCUSING CHARACTERISTICS. COMPARISON WITH PREVIOUS RESULTS

Although the RGS method provides a complete solution to the NLS equation, it is also instructive to discuss integral characteristics of a self-focused beam. The beam critical power P_c is one of the important parameters. It defines a minimum beam power, $P = 2\pi \int I r dr$, required to create a self-focused channel. In the paraxial ray approximation [29] the critical power of a collimated beam reads

$$P_c = \pi c^2 / \gamma \omega^2, \quad (23)$$

while the method of moments [13] predicts a four times larger magnitude

$$P_c^{(m)} = 4P_c = 4\pi c^2 / \gamma \omega^2. \quad (24)$$

Our solution can explain both results, although they correspond to two different physical situations. We found that the equality $\alpha = \beta$ is a necessary condition for the singularity to occur. It coincides with Eq. (23) though the spatial beam structure is quite different from a Gaussian-like beam that the paraxial ray method predicts. This difference is illustrated in Figs. 1 and 2 where the spatial profiles of beam intensity and the phase derivative following from the paraxial ray approximation are plotted as dashed curves. It is seen that both paraxial ray and RGS curves merge in the vicinity of the axis. In particular, the magnitude of the beam on-axis intensity is exactly the same as in the paraxial ray theory. However, the difference between these solutions increases significantly with the radius.

The deficiency of the paraxial ray method is that it assumes the beam does not change its shape. Therefore, the width of the beam tends to zero at the singularity point. Oppositely, the RGS method proves that the on-axis singularity occurs while the beam width remains finite. The method of moments also does not assume the prescribed beam shape, but it defines the beam width in terms of the mean square radius, $\langle r^2 \rangle = 2\pi \int I r^3 dr / P(0)$. For a collimated beam the method of moments identifies the self-focusing threshold as a power where the mean square radius does not depend on z . The mean square radius can also be found by using the RGS solution (11) and (12). The dependence of $\langle r^2 \rangle$ on z is shown in Fig. 5 for the case of a

collimated beam, $R \rightarrow \infty$. Results of the method of moments are also shown for a comparison with dashed lines. One can see that for $\beta < \alpha < 4\beta$ the beam radius calculated from both the RGS and the moments theories monotonically increases with the distance while, according to the paraxial ray theory, the beam power is already above the critical power (23). The difference between our solution and the method of moments is practically negligible, if $\alpha \lesssim 3\beta$ (curve *a*), and the beam radius found from the RGS theory is larger for $\alpha \gtrsim 3\beta$. A qualitative difference in behavior of $\langle r^2 \rangle$ defined from the RGS theory and the method of moments is found for $\alpha > 4\beta$, where according to the moments theory the beam begins to converge and $\langle r^2 \rangle$ decreases monotonically. The RGS theory for this case predicts a nonmonotonous dependence of $\langle r^2 \rangle$ (curve *b* in Fig. 5) which is in agreement with numerical calculations [32]. Only for a very large nonlinearity, $\alpha \gg 4\beta$, does the RGS theory result in a converging value of $\langle r^2 \rangle$. This fact is an indication that this parameter cannot be attributed to the characteristic beam radius and a more appropriate definition of the beam radius is needed. We will introduce it below in the context of the problem of trapped power.

The above comparison of our results with the paraxial ray approximation and the method of moments demonstrates that the RGS method resolves a contradiction in the definition of the critical power: Eq. (23) defines the power where the singularity on the beam axis shows up, while Eq. (24) corresponds to the power where the effective beam radius decreases at least at small distances from the entry plane.

A coordinate dependence of the beam intensity near the singularity point is also a widely discussed characteristic of self-focusing. In general, the RGS solution (11) correlates well with the results of previous studies [27,33,36,38–42,63]: $I(z,0) \propto L(z)/(z_s - z)$, where $L(z)$ is a slow varying function of coordinate z and $z_s = z_{f1}$ is the position of the singularity. However, Eq. (11) predicts that $L(z)$ is a slow algebraic function of z but not a double logarithmic function that has been discussed in [39–42]. This difference is probably due to the Gaussian boundary condition used in our RGS solution. Such a slow algebraic dependence is similar to that which has been obtained for an exact explosive solution to the NLS equation with a different boundary condition in Ref. [59].

One of the most important characteristics of self-focusing is the amount of power trapped in a singularity. Since the rays that enter the singularity are excluded from consideration, the beam power in the off-axis region, $r > 0$ (i.e., $\chi^2 > \chi_b^2$), $P(z) = 2\pi \int_0^\infty r I(z,r) dr$, decreases with z . Correspondingly, we define the trapped power part as $p_{tr}(z) = 1 - P(z)/P(0)$ where $P(0)$ is the incident beam power. It is also instructive to define the effective beam radius, $r_{tr}(z)$, as a radius that encircles half of the incident power, $2\pi \int_{r_{tr}}^\infty I r dr = P(0)/2$.

Algebraic expressions can be written for the trapped power and the effective beam radius from Eqs. (11) and (12). The trapped power part, $p_{tr}(z)$, has to be found from the equation

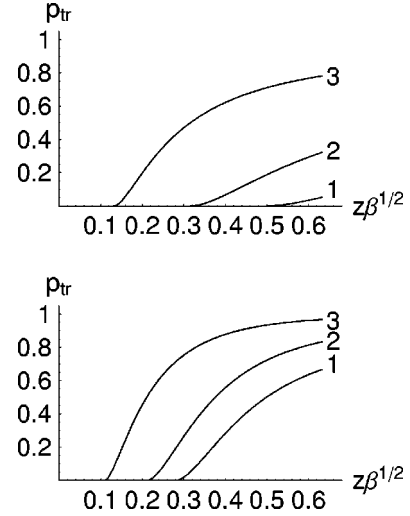


FIG. 6. Axial dependence of the trapped power part p_{tr} for a collimated beam (upper panel) and a focused beam with $R=20$ (bottom panel) in a medium with $\beta=0.001$ and $\alpha/\beta=3$ (1), 6 (2), and 30 (3).

$$\ln \frac{1}{1-p_{tr}} + \frac{\alpha}{\beta}(1-p_{tr}) = \left[1 + \frac{(1-z/R)^2}{2\beta z^2} \right] \times \left[1 + \ln \frac{2\alpha z^2}{2\beta z^2 + (1-z/R)^2} \right]. \quad (25)$$

The effective beam radius is defined by the following relation:

$$r_{tr} = \sqrt{\lambda} \left(1 - \frac{z}{R} \right) \left[1 + \frac{2\beta z^2}{(1-z/R)^2} \left(1 - \frac{\alpha}{\beta} e^{-\lambda} \right) \right], \quad (26)$$

where the function $\lambda(z)$ has to be found from the equation

$$\frac{\beta}{\alpha}(\lambda - \ln 2) + e^{-\lambda} + \frac{2\lambda\alpha z^2}{(1-z/R)^2} \left(\frac{\beta}{\alpha} - e^{-\lambda} \right)^2 = \frac{1}{2}. \quad (27)$$

Figures 6 and 7 demonstrate the z dependence of p_{tr} and r_{tr} for different values of the ratio $\alpha/\beta = P(0)/P_c$. In Fig. 6 the point where p_{tr} departs from zero is the singularity point. It moves closer to the entrance as the beam power increases. The trapped power increases with z as more rays enter the singularity. It also increases with the beam power. One can see in Fig. 6(a) that for a collimated beam with $\alpha/\beta=3$ the trapped power approaches 67% for $z \rightarrow \infty$ while for $\alpha/\beta=30$ the trapped power reaches 97%. This is an important result of analytic theory which quantifies the amount of energy trapped in the channel. Our analysis for a converging beam is restricted by the length of the geometrical optics focus, $z \leq R$. It is demonstrated in Fig. 6(b) that for $\alpha \gg \beta$ the trapped power near the geometrical optics focus, $z=R$, is also comparable to the total incident power. The trapped power at the geometrical optics focus $p_{tr}(R)$ might be con-

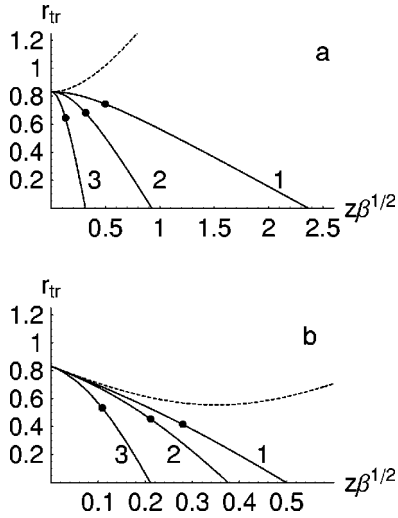


FIG. 7. Axial dependence of the effective beam radius r_{tr} for a collimated beam (a) and a focused beam with $R=20$ (b) in a medium with $\beta=0.001$ and $\alpha/\beta=3$ (1), 6 (2), and 30 (3). The dots on the curves mark the position of singularity. The linear solution, $\alpha=0$, is shown with a dashed line.

sidered as a global characteristic of a converging beam self-focusing. Using the analytical solution (25) for $z=R$ one finds

$$p_{tr}(R) = 1 - \frac{\beta}{\alpha} \equiv 1 - \frac{P_c}{P(0)}. \quad (28)$$

That is, the trapped power is equal to the incident beam power with the exception of the critical power. This conclusion is in an apparent contradiction with a heuristic expectation that the critical power should be trapped in a channel while the rest of the incident power could be radiated. It would be interesting to investigate whether this result is specific for a cubic nonlinearity and a Gaussian incident beam profile or if it has a more general significance.

The effective beam radius in Fig. 7 decreases with the distance which is also an indication of self-focusing. The distance l_{tr} , where r_{tr} equals zero, can be considered as a self-trapping length, which is a length where 50% of the beam power is trapped. The condition $r_{tr}=0$ applied to Eq. (26) defines the following expression for the self-trapping length:

$$l_{tr} = \frac{R}{1 + R\sqrt{2(\alpha e^{-\kappa} - \beta)}} \quad \text{where} \quad \frac{1}{2} + \frac{\beta}{\alpha} \ln 2 = (1 + \kappa)e^{-\kappa}. \quad (29)$$

The dependence of the self-trapping length on the beam power and the wave-front curvature is shown in Fig. 8. In the limit of high intensity, $\alpha/\beta \gg 1$, the self-focusing length has a simple asymptotics: $l_{tr} \approx 1.6\alpha^{-1/2}$.

V. SUMMARY

An important result of the RGS theory consists of an analytical solution to the BVP problem for a NLS equation with

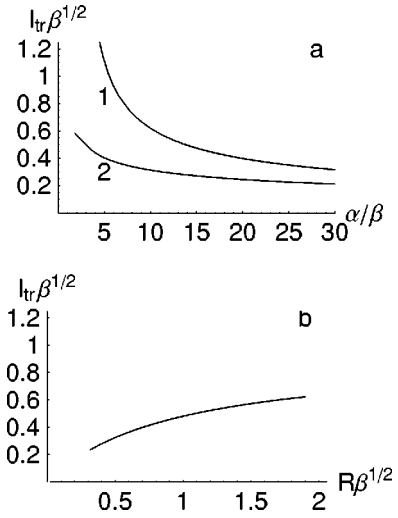


FIG. 8. Upper panel: dependence of the self-focusing length $\sqrt{\beta}l_{tr}$ on α/β for a collimated beam (curve 1) and a focused beam (curve 2) with the curvature $\sqrt{\beta}R=20$. Bottom panel: dependence of the self-focusing length on the wavefront curvature, $\sqrt{\beta}R$, for $\alpha/\beta=6$.

a cubic nonlinearity and a Gaussian beam profile at the entrance boundary. It provides a quantitative description of the beam electric field everywhere in a nonlinear media and allows us to define the global self-focusing characteristics in a more accurate way. In particular, we explain a contradiction in the definition of the critical power between the paraxial ray approximation and the method of moments. We also suggest another definition for the effective beam radius and the self-focusing length and compare them with the previous definitions. Our solution indicates also that the singularity at the beam intensity shows up at low powers, before the whole beam starts to converge, and the asymptotic behavior of the light intensity near the singularity depends on the incident beam profile. The RGS solution allowed us to derive a parametric scaling for self-focusing. It predicts the dependence of the trapped power and the length of self-focusing on the nonlinearity, diffraction, and the wave-front curvature.

The assumptions about the Gaussian profile of the incident beam, axial symmetry, and a cubic nonlinearity are not restrictive. The RGS method is more general and can be applied to arbitrary boundary data, another type of nonlinearity, and to an inhomogeneous medium. The Gaussian beam profile provides an instructive example which has a long history and can be compared with a number of previously published results. Such a comparison demonstrates advantages of the RGS method as a tool for the nonlinear electrodynamics.

ACKNOWLEDGMENTS

This work was supported in part by the International Science and Technology Center, Project No. 310-96 and the Russian Foundation for Basic Research (Grants No. 98-02-17385-a and No. 99-01-00232).

- [1] G. A. Askar'yan, Zh. Éksp. Teor. Fiz. **42**, 1083 (1962) [Sov. Phys. JETP **15**, 1567 (1962)].
- [2] R. Chiao, E. Garmire, and G. Townes, Phys. Rev. Lett. **13**, 479 (1964); **14**, 1056 (1965); **16**, 347 (1966).
- [3] V. I. Talanov, Zh. Éksp. Teor. Fiz. Pis'ma Red. **2**, 218 (1965) [JETP Lett. **2**, 138 (1965)].
- [4] S. A. Akhmanov, A. P. Sukhorukov, and R. V. Khokhlov, Zh. Éksp. Teor. Fiz. **50**, 1537 (1966) [Sov. Phys. JETP **23**, 1025 (1966)].
- [5] A. L. Dyshko, V. N. Lugovoi, and A. M. Prokhorov, Zh. Éksp. Teor. Fiz. Pis'ma Red. **6**, 655 (1967) [JETP Lett. **6**, 146 (1967)].
- [6] P. Sprangle, E. Esarey, J. Krall, and G. Joyce, Phys. Rev. Lett. **69**, 2200 (1992).
- [7] S. V. Bulanov, F. Pegoraro, and A. M. Pukhov, Phys. Rev. Lett. **74**, 710 (1995).
- [8] P. Mora and T. M. Antonsen, Jr., Phys. Rev. E **53**, 2068 (1996).
- [9] V. E. Zakharov and A. B. Shabat, Zh. Éksp. Teor. Fiz. **61**, 118 (1971) [Sov. Phys. JETP **34**, 62 (1972)].
- [10] V. B. Taranov, Institute for Nuclear Research Report No. KIYaI-80-15, 1980; J. Plasma Phys. **35**, 141 (1986).
- [11] L. Gagnon and P. Winternitz, J. Phys. A **21**, 1493 (1988); **22**, 469 (1989); L. Gagnon, B. Grammaticos, A. Ramani, and P. Winternitz, *ibid.* **22**, 499 (1989).
- [12] M. S. Sodha, A. K. Ghatak, and V. K. Tripathi, in *Progress in Optics*, edited by E. Wolf (North-Holland, Amsterdam, 1976), Vol. XIII, pp. 171–265.
- [13] S. N. Vlasov, V. A. Petrishchev, and V. I. Talanov, Radiophys. Quantum Electron. **14**, 1062 (1974).
- [14] D. Anderson and M. Bonnedal, Phys. Fluids **22**, 105 (1979).
- [15] V. E. Zakharov and S. V. Manakov, Zh. Éksp. Teor. Fiz. **71**, 203 (1976) [Sov. Phys. JETP **44**, 106 (1976)].
- [16] R. H. Enns and S. S. Rangnekar, Can. J. Phys. **63**, 632 (1985).
- [17] L. Bergé, Phys. Rep. **303**, 259 (1998).
- [18] V. F. Kovalev, V. V. Pustovalov, and D. V. Shirkov, J. Math. Phys. **39**, 1170 (1998).
- [19] V. E. Zakharov, S. V. Manakov, S. P. Novikov, and L. P. Pitaevskij, *Soliton Theory: Inverse Scattering Method* (Nauka, Moscow, 1980) (in Russian).
- [20] V. A. Andreev, *Inverse Scattering Method in Quantum Optics Equations. II. Singular and Radiation Solutions*, Proceedings of the Lebedev Physical Institute Vol. 211 (Nauka, Moscow, 1991), pp. 3–37 (in Russian).
- [21] L. Gagnon and P. Winternitz, Phys. Lett. A **134**, 276 (1989); J. Phys. A **25**, 4425 (1992); Phys. Rev. A **39**, 296 (1989).
- [22] V. M. Eleonskii and V. P. Silin, Zh. Éksp. Teor. Fiz. **56**, 574 (1969) [Sov. Phys. JETP **29**, 317 (1969)].
- [23] C. E. Max, Phys. Fluids **19**, 84 (1976).
- [24] J. L. Francisco, B. Lippmann, and F. Tappert, Phys. Fluids **20**, 1176 (1977).
- [25] S. A. Akhmanov, A. P. Sukhorukov, and R. V. Khokhlov, Usp. Fiz. Nauk **93**, 19 (1967) [Sov. Phys. Usp. **10**, 609 (1968)].
- [26] A. V. Gurevich and A. B. Shvartsburg, *Nonlinear Theory of Radiowave Propagation in the Ionosphere* (Nauka, Moscow, 1973) (in Russian).
- [27] D. Wood, Stud. Appl. Math. **71**, 103 (1984).
- [28] K. Rypdal, J. J. Rasmussen, and K. Thomsen, Physica D **16**, 339 (1985).
- [29] M. B. Vinogradova, O. V. Rudenko, and A. P. Sukhorukov, *Theory of Waves* (Nauka, Moscow, 1973) (in Russian).
- [30] Z. K. Yankauskas, Izv. Vyssh. Uchebn. Zaved. Radiofiz. **9**, 412 (1966) [Sov. Radiophys. **9**, 261 (1966)].
- [31] H. A. Haus, Appl. Phys. Lett. **8**, 128 (1966).
- [32] V. N. Gol'dberger, V. I. Talanov, and R. E. Erm, Izv. Vyssh. Uchebn. Zaved. Radiofiz. **10**, 674 (1967) [Sov. Radiophys. **10**, 427 (1967)].
- [33] D. W. McLaughlin, G. C. Papanicolaou, C. Sulem, and P. L. Sulem, Phys. Rev. A **32**, 1200 (1986); P. L. Sulem, C. Sulem, and A. Patera, Commun. Pure Appl. Math. **37**, 755 (1984).
- [34] N. E. Andreev, L. M. Gorbunov, A. I. Zykov, and E. V. Chizhonkov, Zh. Éksp. Teor. Fiz. **106**, 1676 (1994) [JETP **79**, 905 (1994)].
- [35] N. E. Kosmatov, V. E. Zakharov, and V. F. Shvets, Physica D **52**, 16 (1991).
- [36] S. N. Vlasov, L. V. Piskunova, and V. I. Talanov, Zh. Eksp. Teor. Fiz. **75**, 1602 (1978) [Sov. Phys. JETP **48**, 808 (1978)]; S. N. Vlasov and V. I. Talanov, in *Nonlinear Waves: Dynamics and Evolution*, (Nauka, Moscow, 1989), p. 218 (in Russian).
- [37] F. H. Berkshire and J. D. Gibbon, Stud. Appl. Math. **69**, 229 (1983).
- [38] K. Rypdal and J. J. Rasmussen, Phys. Scr. **33**, 481 (1986).
- [39] B. J. LeMesurier, G. C. Papanicolaou, C. Sulem, and P. L. Sulem, Physica D **32**, 210 (1988).
- [40] G. M. Fraiman, Zh. Éksp. Teor. Fiz. **88**, 390 (1985) [Sov. Phys. JETP **61**, 228 (1985)].
- [41] V. M. Malkin, Phys. Lett. A **151**, 285 (1990).
- [42] L. Bergé and D. Pesme, Phys. Lett. A **166**, 116 (1992).
- [43] V. I. Talanov, Izv. Vyssh. Uchebn. Zaved. Radiofiz. **9**, 410 (1966) [Sov. Radiophys. **9**, 260 (1966)].
- [44] E. E. C. Stueckelberg and A. Petermann, Helv. Phys. Acta **22**, 499 (1953); M. Gell-Mann and F. Low, Phys. Rev. **95**, 1300 (1954); N. N. Bogoliubov and D. V. Shirkov, Dokl. Akad. Nauk SSSR **103**, 203 (1955); **103**, 391 (1955); Nuovo Cimento **3**, 845 (1956).
- [45] K. Wilson, Phys. Rev. B **4**, 3174 (1971); P. G. de Gennes, Phys. Lett. A **38**, 339 (1972); J. Zinn-Justin, *Quantum Field Theory and Critical Phenomena* (Clarendon Press, Oxford, 1978).
- [46] D. V. Shirkov, Dokl. Akad. Nauk SSSR **263**, 64 (1982) [Sov. Phys. Dokl. **27**, 197 (1982)]; Theor. Math. Phys. **60**, 778 (1984).
- [47] V. F. Kovalev and V. V. Pustovalov, Theor. Math. Phys. **81**, 1060 (1990); Sov. Phys. Lebedev. Inst. Rep. **3**, 54 (1989).
- [48] N. Goldenfeld, O. Martin, and Y. Oono, J. Sci. Comput. **4**, 355 (1989).
- [49] J. Bricmont, A. Kupiainen, and J. Xin, J. Diff. Eqns. **130**, 9 (1996).
- [50] L.-Y. Chen, N. Goldenfeld, and Y. Oono, Phys. Rev. E **54**, 376 (1996).
- [51] D. V. Shirkov, in *Proceedings of Second International Conference, Dubna, USSR, 1991* edited by D. V. Shirkov and V. B. Priezhev (World Scientific, Singapore, 1992), p. 1; V. F. Kovalev, S. V. Krivenko, and V. V. Pustovalov, *ibid.*, p. 300.
- [52] V. F. Kovalev, in *Proceedings of the Third International Conference "Renormalization Group 96," Dubna, 1996*, edited by D. V. Shirkov, D. I. Kazakov, and V. B. Priezhev (Joint Institute for Nuclear Research, Dubna, 1997), p. 263.

- [53] V. F. Kovalev, V. V. Pustovalov, and S. I. Senashov, *Diff. Equations* **29**, 1521 (1993).
- [54] V. F. Kovalev, *J. Nonlinear Math. Phys.* **3**, 351 (1996).
- [55] V. F. Kovalev and V. V. Pustovalov, *Math. Comput. Modeling* **25**, 165 (1997).
- [56] V. F. Kovalev, *Theor. Math. Phys.* **111**, 686 (1997).
- [57] V. F. Kovalev and D. V. Shirkov, *J. Nonlinear Opt. Phys. Mater.* **6**, 443 (1997).
- [58] V. A. Baikov, R. K. Gazizov, and N. H. Ibragimov, *J. Sov. Math.* **55**, 1450 (1991).
- [59] V. F. Kovalev, *Theor. Math. Phys.* **119**, 719 (1999).
- [60] P. Kaw, G. Schmidt, and T. Wilcox, *Phys. Fluids* **16**, 1522 (1973).
- [61] V. N. Lugovoi and A. M. Prokhorov, *Usp. Fiz. Nauk* **111**, 203 (1973) [*Sov. Phys. Usp.* **16**, 658 (1974)].
- [62] A. V. Brantov, V. Yu. Bychenkov, V. T. Tikhonchuk, and W. Rozmus, *Phys. Plasmas* **5**, 2742 (1998).
- [63] R. T. Glassey, *J. Math. Phys.* **18**, 1794 (1977).